

# Deep Rolling of Al6061-T6 Material and Performance Evaluation with New Type Designed WNMG Formed Rolling Tool

Oktaı Adıyaman<sup>1\*</sup> , Feyza AYDIN<sup>2</sup> 

<sup>1,2</sup> Batman University, Institute Of Graduate Studies, Batman, Türkiye

\*[oktay.adiyaman@batman.edu.tr](mailto:oktay.adiyaman@batman.edu.tr)

\* Orcid No: 0000-0002-2674-3836

Received: 17 December 2023

Accepted: 15 March 2024

DOI: 10.18466/cbayarfbe.1405976

## Abstract

In deep rolling, ball and roller type burnishing tools are generally used. It is generally difficult to deep roll contours with curved and conical shapes with the existing rolling tools. The aim of this study is to design experiments with a roller insert that will be an alternative to deep rolling inserts being used now and that can be fixed on the present tool holders; and to investigate the usability of them including curve and conical formed workpieces with the help of this designed tool. For this purpose, a spherical insert with a radius of 1 mm in the form of WNMG was designed based on the WNMG insert model and used in deep rolling of Al6061-T6 material using different forms and parameters. 143, 330, 495 N rolling force, 0.04, 0.08, 0.12 mm/rev feed and 400, 600, 800 rpm spindle speed were selected as rolling parameters. By examining the microhardness and surface structure of deep-rolled Al6061 parts, the achievability of the results of existing tools in deep rolling was investigated. At the end of the study, it was determined that the new type of rolling tool produced results similar to the existing tools in deep rolling in terms of microhardness and surface morphology, which enabled that the workpieces with curve and conical forms could also be rolled, and that this rolling tool could be used as an alternative in deep rolling.

**Keywords:** Al6061, deep rolling, microhardness, surface roughness, tribology

## 1. Introduction

In order to correct the negative effects on the machined surfaces of the materials, many finishing applications such as grinding, honing, lapping [1], and ultrasound-aided deep rolling [2] are used. Prabhu et al. divided the methods applied for surface smoothing into two main categories. The first of these is the method that involves material loss, such as grinding method, while the second is the method that works by redistributing the material on the surface and plastic compression of the surface and does not involve material loss, such as ball burning and deep rolling methods [3].

The process of smoothing the surfaces of the machined parts by rolling them without removing any chips from their surfaces is defined as rolling. After the rolling process, the surface quality (Ra, etc.) of the work pieces is improved, as well as the mechanical properties of the workpieces, such as microhardness, fatigue resistance, wear resistance. Thanks to this treatment role of the rolling process, this method is preferred more than the

other surface improvement methods such as grinding [4]. In order to improve the surfaces of the machined elements, the deep rolling technique, which is based on the plastic deformation of the surfaces without removing the chips by means of a rolling insert or roller, is mostly applied to the inner and outer surfaces of the turned and ground workpieces [5, 6]. As a result of the process, the surface roughness (Ra) of the material decreases significantly, and the surface hardness increases. Additionally, at the end of the process, the tensile strength on the surface turns into compressive stresses, resulting in a high improvement in fatigue life [7]. Deep rolling process can be applied to steel materials as well as other light metals (brass, aluminum (Al), etc.).

In addition to the studies investigating the effect of process parameters on the results, there are also similar studies on the tools used in rolling. For this purpose, the effects of three different apparatus designed for using different parameters (rolling force, feed and number of passes) and the process parameters were investigated, and compared depending on the surface hardness and Ra

of Al-6061-T6 material. It was observed that the best Ra and surface hardness values were obtained with the apparatus with a ball-rolling insert [4].

Studies on deep and ball rolling were also applied to aluminum and its alloys. Analysis and research were carried out on the application of the rolling process of Al and its alloys, both on cylindrical surfaces in turning applications [8-14] and on planar surfaces in milling applications [15-17]. The circularity of the inner surfaces of hole was examined and compared with the machining methods in terms of Ra after rolling [18]. In another similar study [19], changes in Ra, microstructure and surface hardness of the inner surface of the hole of Al-6061 alloy were compared as a result of different machining methods such as drilling, internal turning, hole-grinding, honing, reaming and deep rolling processes. In addition, the effects of the process parameters (rolling pressure and number of passes) applied in the rolling method on fatigue, residual stress, microhardness and Ra were investigated experimentally. It was determined that ball rolling method improved the Ra; and the number of passes had a 41% effect on Ra. It was determined that the applied force and number of passes increased the microhardness of the material, and depending on the increase in force and number of passes, the microhardness of the workpiece increased by approximately 20 Hv. It was established that with the increase in rolling force, the subsurface residual stress in the material also increased. It was seen that not only the fatigue strength was improved but also the fatigue life was increased [18]. In addition to the effect of process parameters on the results, there are also similar studies on the tools used in rolling. For this purpose, the effects of three different apparatus designed for using different parameters (rolling force, feed and number of passes) and the process parameters were investigated and compared depending on the surface hardness and surface roughness of Al-6061-T6 material. It was observed that the best Ra and surface hardness were obtained with the apparatus with a ball-rolling insert [4]. In a different study, the effect of the rolling insert at different diameters was examined, and the surface of 5083 Al-Mg material was subjected to rolling using different parameters with ball diameters of 11.112 mm, 13.494 mm, 15.081 mm and 16.669 mm [20]. Regarding the rolling process applied in the form of milling application, the polishing process was carried out by using different process parameters with a simple rolling tool [21], and the resulting residual stresses were examined and the results were compared with the results in the numerical analysis program. It was established that there were compressive residual stresses on all rolled surfaces. Besides the process parameters, the effect of rolling direction and lubricant usage was also examined.

The analysis of the method continues in many different ways such as studies on deep rolling including simulation studies [22], analysis of deep rolling with the finite

element method [23,24], testing of deep rolling applications in different working environments (e.g. cryogenic) [23] and deep rolling with rolling tools of different diameters using methods such as regression, response surface method (RSM), ANOVA etc. [3, 25-30], Blasón et al. examined the strength increase of D38MnV5 S steel with a roller type toll [31].

There are many parameters that affect the results obtained in deep rolling method. It is both difficult and complex to examine the effects of these parameters on each mechanical property of the material simultaneously. In order to save time and cost in studies, Taguchi orthogonal experimental design method is one of the preferred methods instead of full factorial experimental design [7, 32, 3]. With Taguchi DOE, the number of experiments can be reduced and the effect of the parameters on the results can be examined. In addition, the subject can be examined with analyzes such as Artificial Neural Networks (ANN) [27], Response Surface Methodology (RSM) etc. [33].

When all previous studies were examined, it was observed that in majority of the studies, ball and roller type rolling tools were used; and generally, flat contours were deep rolled. In a previous study [34, 35], deep rolling process was applied to Al6061-T6 material with the designed rolling tool; thus, the effect of rolling parameters (speed, rolling pressure and feed) on the surface roughness obtained on conical and cylindrical surfaces was investigated. In this study, deep rolling process was applied to the cylindrical and conical surfaces of Al6061-T6 material with the designed and manufactured rolling insert, and as a result, the effects of the parameters on microhardness and surface morphology were investigated.

## 2. Materials and Methods

All turning operations were performed on a SMARC model CAK6166B X 200 CNC lathe. According to process, planning and process steps are shown in Figure 1.

The design of the rolling tool was referenced on WNMG 080408 type insert used in the industry, and a WNMG type rolling insert with a spherical nose shape and 1 mm radius was manufactured. Polishing process was applied to the spherical nose and friction was minimized (Figure 2).

A special tool holding apparatus was designed to fix the spherical edged rolling insert with the radius shown in Figure 2, and the tool holder to which this insert will be mounted to the turret of the CNC lathe machine for use in deep rolling with different rolling pressures (Figure 3 a), and then rolling process was carried out. (Figure 3 b). The rolling force was adjusted by moving the pressure adjustment spring length with the pre-load thread (Figure 3 a).



In this paper, Taguchi experimental design was preferred as the experimental design and analysis method. L27 orthogonal design was used in the experiments and combinations were created. Three parameters in total and, in connection with them, 3 levels were determined for each parameter (Table 3). For the microhardness measurements of the test samples, samples were taken from cylindrical and conical surfaces and the microhardness values of these samples were measured with AOB brand Vickers microhardness device. Measurements were taken according to the Vickers hardness measurement method and applied under a load of 30 g. On each sample, 3 hardness measurements of cylindrical and conical surfaces from different points (Figure 4 a) and 3 measurements were taken from the radial, and then the arithmetic mean of these values was recorded as the hardness value of that sample (Figure 4).

**Table 3.** L27 experimental design

| Exp. No | Rolling Force (N) | Feed (mm/rev) | Spindle Speed (rpm) |
|---------|-------------------|---------------|---------------------|
| 1       | 143               | 0.04          | 400                 |
| 2       | 143               | 0.08          | 400                 |
| 3       | 143               | 0.12          | 400                 |
| 4       | 143               | 0.04          | 600                 |
| 5       | 143               | 0.08          | 600                 |
| 6       | 143               | 0.12          | 600                 |
| 7       | 143               | 0.04          | 800                 |
| 8       | 143               | 0.08          | 800                 |
| 9       | 143               | 0.12          | 800                 |
| 10      | 330               | 0.04          | 400                 |
| 11      | 330               | 0.08          | 400                 |
| 12      | 330               | 0.12          | 400                 |
| 13      | 330               | 0.04          | 600                 |
| 14      | 330               | 0.08          | 600                 |
| 15      | 330               | 0.12          | 600                 |
| 16      | 330               | 0.04          | 800                 |
| 17      | 330               | 0.08          | 800                 |
| 18      | 330               | 0.12          | 800                 |
| 19      | 495               | 0.04          | 400                 |
| 20      | 495               | 0.08          | 400                 |
| 21      | 495               | 0.12          | 400                 |
| 22      | 495               | 0.04          | 600                 |
| 23      | 495               | 0.08          | 600                 |
| 24      | 495               | 0.12          | 600                 |
| 25      | 495               | 0.04          | 800                 |
| 26      | 495               | 0.08          | 800                 |
| 27      | 495               | 0.12          | 800                 |

In order to view the surface properties of deep rolled surfaces, surface images were taken with an optical microscope. In the optical photographs taken, horizontal lines represent the direction perpendicular to the workpiece axis. Optical photographs were taken from the vertices of cylindrical surfaces. SEM analyzes were carried out to examine the carbide, groove, scratch and microstructures of the deep rolled surfaces in more detail. For this purpose, images were taken using the SEM device.

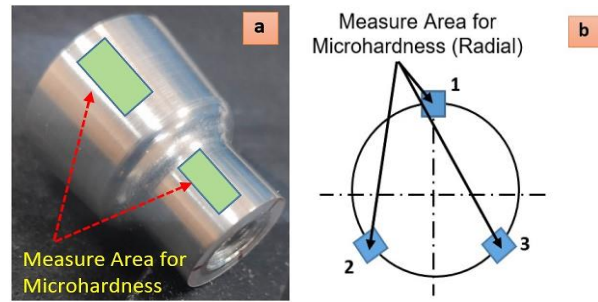


**Figure 4.** Measure of microhardness

### 3. Results and Discussion

According to the designed insert and the results of the previous study [34, 35] on the processing of Al6061-T6 material with this insert and Ra, it was found that the ideal parameter for Ra is 495 N in rolling force, 0.12 mm/rev in feed value and 600 rev in rotational speed. In addition, it was determined that the newly designed insert was suitable for using in deep rolling and could be used in conical, radius and longitudinal rolling operations at the same time. It was found that the most effective parameter on Ra was the feed value [34, 35]. Microhardness measurement values obtained from deep rolling test samples are given in Table 4.

**Table 4.** Values of microhardness

| Exp. No | A | B | C | Microhardness (Hv <sub>0.3</sub> ) |
|---------|---|---|---|------------------------------------|
| 1       | 1 | 1 | 1 | 158                                |
| 2       | 1 | 2 | 1 | 163.53                             |
| 3       | 1 | 3 | 1 | 165.26                             |
| 4       | 1 | 1 | 2 | 154.8                              |
| 5       | 1 | 2 | 2 | 164.1                              |
| 6       | 1 | 3 | 2 | 169.6                              |
| 7       | 1 | 1 | 3 | 162.73                             |
| 8       | 1 | 2 | 3 | 163.7                              |
| 9       | 1 | 3 | 3 | 158.76                             |
| 10      | 2 | 1 | 1 | 164.46                             |
| 11      | 2 | 2 | 1 | 173.26                             |
| 12      | 2 | 3 | 1 | 164.86                             |
| 13      | 2 | 1 | 2 | 151.8                              |
| 14      | 2 | 2 | 2 | 165.66                             |
| 15      | 2 | 3 | 2 | 158.63                             |
| 16      | 2 | 1 | 3 | 167.13                             |
| 17      | 2 | 2 | 3 | 155.9                              |
| 18      | 2 | 3 | 3 | 160.7                              |
| 19      | 3 | 1 | 1 | 168.1                              |
| 20      | 3 | 2 | 1 | 159.53                             |
| 21      | 3 | 3 | 1 | 161.46                             |
| 22      | 3 | 1 | 2 | 165.4                              |
| 23      | 3 | 2 | 2 | 174.7                              |
| 24      | 3 | 3 | 2 | 164.96                             |
| 25      | 3 | 1 | 3 | 162.63                             |
| 26      | 3 | 2 | 3 | 156.86                             |
| 27      | 3 | 3 | 3 | 157.5                              |

In Table 4, symbols A, B and C express rolling force (N), feed (mm/rev) and spindle speed (rpm), respectively. The numbers 1, 2 and 3 express the level of each parameter. Before the statistical analysis, it was analyzed whether the microhardness values obtained in Table 4 showed a normal distribution; hence, the graph in Figure 5 was obtained.

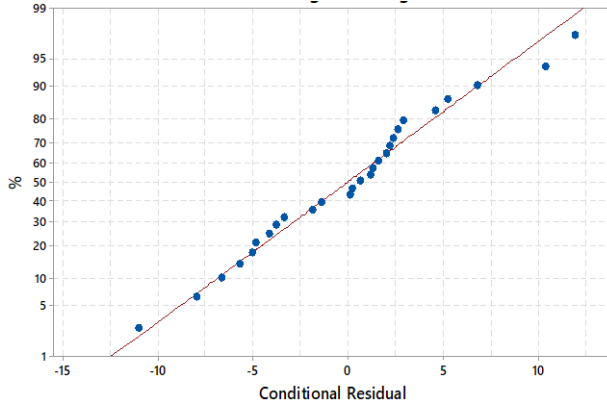


**Figure 5.** Probability of microhardness

The results obtained (Figure 5) show a normal distribution. It is known that surface hardness increases on surfaces subjected to rolling [33, 7]. In this study, the increase in microhardness values was measured before and after the rolling process in order to observe this effect of rolling. The graphical representation of the measurement results can be seen in the graph in Figure 6.

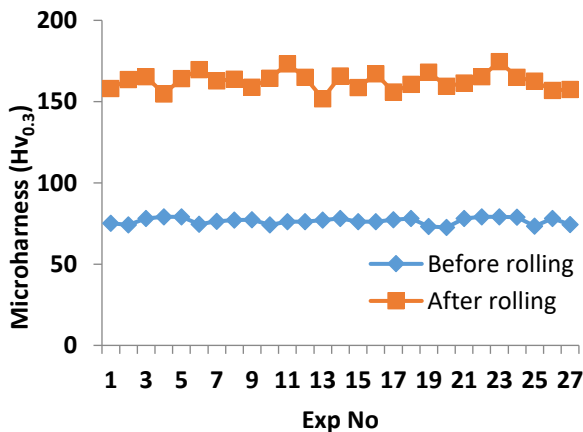


**Figure 6.** Microhardness graph before and after rolling

The microhardness values, which were in the range of 70-75  $Hv_{0.3}$  before rolling, increased by nearly 100% with the effect of rolling, thus hardness values in the range of 160-180  $Hv_{0.3}$  were obtained (Figure 6). From this, it can be concluded that rolling process increases the surface hardness under all conditions. Tayeb et al. stated that when the rolling polishing process was applied to Al6061 material, they found a microhardness of 78-92 HRB (150-200 Hv) depending on different process parameters [41]. Egea et al. found that the surface hardness of Al2050 material increased by 37.5% after rolling and

polishing, resulting in a micro hardness value of 140-160 Hv [42]. In his study, Koçak found a 10% hardness increase for Al6013 material and a 20% hardness increase for MS 58 material. The microhardness values found after the process are similar to the values in the literature [43, 18, 7]. Akkurt and Ovalı [18] obtained the hardness value in the range of 110-130  $Hv_{0.01}$  in deep rolling of Al6061 material. Additionally, Akyuz [7] obtained hardness values as 160-180  $Hv_{0.02}$  in deep rolling of AA7075-T6 material. Axir et al. [33] obtained hardness values in the range of 180-230 Hv for Al alloy 2014 material. The alloying of Al material with different metals is a phenomenon that also increases the hardness value [33]. Signal noise analysis was performed to see at what level the process parameters affected the micro hardness values obtained. In calculating the signal-to-noise (S/N) ratio, the "greatest is best" principle was taken as reference. The graph obtained from this analysis is seen in Figure 7.

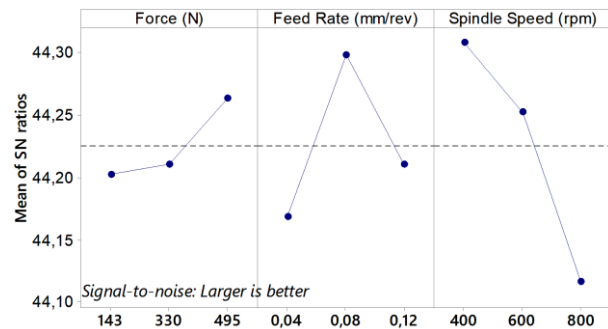


**Figure 7.** Plot of signal to noise ratios

The graph affecting microhardness is shown in Figure 7. As Figure 7, the most ideal parameter values on Ra are 495 N in rolling force, 0.08 mm/rev in feed, and 400 rpm in number of revolutions. In the experiments where the rolling pressure was 495 N, it was observed that hardness increased above the occurred average values, but hardness values below the average occurred at 143 N and 330 N. In terms of feed, it can be said that the values of 0.04 mm/rev and 0.12 mm/rev did not constitute the desired value in terms of hardness and that the value of 0.08 mm/rev was the optimum level for hardness. It is seen that there is an inverse proportion between the spindle speeds and the hardness. Here, it was concluded that there was an increase in hardness due to friction-related temperature and this value was obtained at 400 rpm. In order to see the change between processing parameters and microhardness, the evaluations were made; hence, the graphs in Figure 8 were obtained.

When previous studies on deep rolling are examined, it is seen that a definitive relationship between microhardness and process parameters cannot be obtained in most studies. This result is mostly similar for Figure 8 as well. When all parameters and parameter levels and both Ra and microhardness results are evaluated together, it is seen that the most important problem in the studies in the

literature, the inability to reach definite conclusions, has emerged the same as in our study. Although general conclusions have been obtained, further studies on ball and deep rolling are required to form conclusions with accuracy similar to those in surface smoothing operations such as machining or grinding.

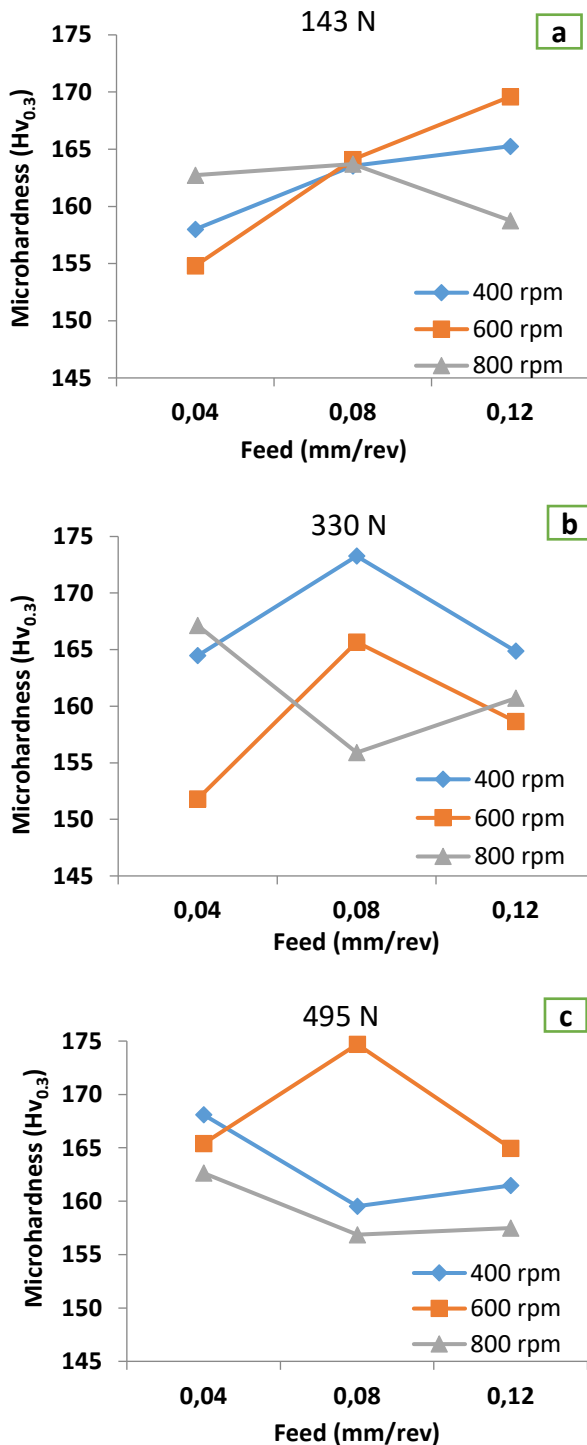


**Figure 8.** Relationship graph between machining parameters and microhardness

Axir et al. [33] observed that with the increase in feed and number of passes, microhardness increases up to certain values (for feed: 0.015 to 0.035 mm/rev and for the number of passes: 1 to 3) and then decreases.

Similarly, Basak et al. [27] obtained hardness values between 150-190 Hv at different rolling forces (100 N to 400 N) in the rolling of Al-Mg alloy. They observed that the increase in rolling force and feed caused an increase in hardness.

### 3.1 Optical Microscope Images

In order to examine the surface properties after deep rolling, both optical microscope images and SEM images were taken. In optical photographs, the horizontal lines represent the direction perpendicular to the workpiece axis. Optical photographs were taken from the top points of cylindrical surfaces. The surface image with finish turning operation before rolling is seen in Figure 9.

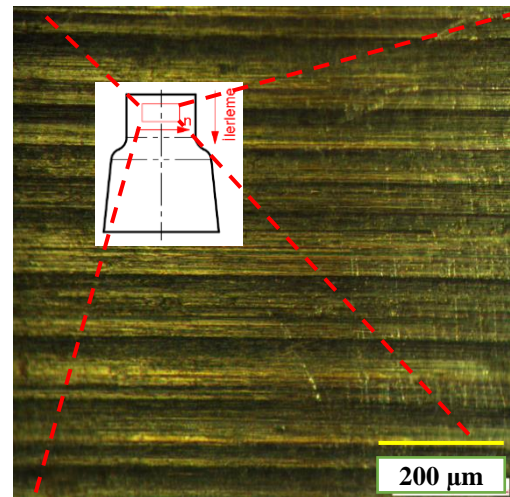


**Figure 9.** Surface optic view before deep rolling

When Figure 9 is examined, it can be seen that the normal appearance that is generally seen in the literature [44, 18, 45] as a result of the turning operation is also formed here. The images in Figure 10 were obtained from the images obtained after rolling.

The samples were taken at 200x magnification as shown in Figure 9 and Figure 10. In the images, it can be seen that the particles are generally distributed homogeneously. It is seen that Al6061 aluminum alloy has micro-pores of small sizes. When looking at the microscope images in Figure 10, it is seen that the bright surfaces are brighter because they are in the shape of cylindrical surfaces, while the dark areas are subject to erosion in the form of deep grooves. In deep rolling, debris and grooves may occur due to friction. Surface irregularities such as debris, grooves etc. have also been found by different researchers [46, 47]. Generally, the surface structure seen in Figure 10 in deep rolling is also

seen in previous studies [48, 49]. Additionally, when Figure 10 is examined, it is clearly seen that deformations occur on the surface as the feed rate increases. In the literature [3], it is stated that surface roughness increases as the pressure force increases in deep rolling.

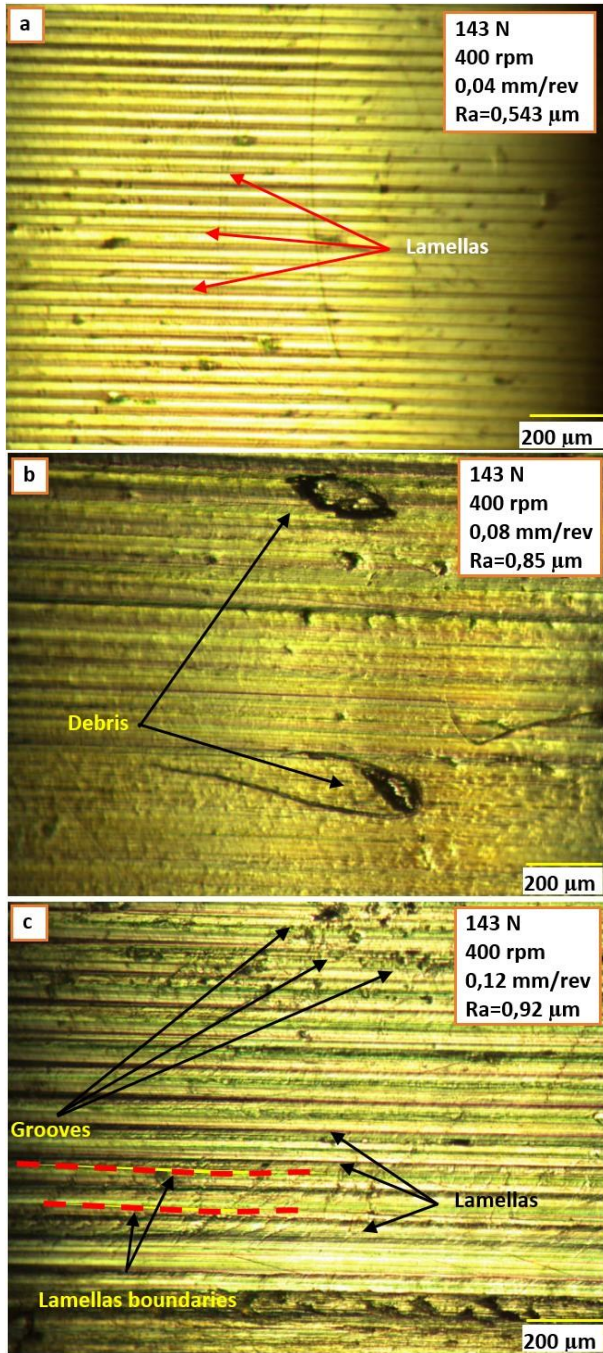


**Figure 10.** Optical photographs obtained at a rolling force of 143 N a) Ra=0,543 b) Ra=0,85 c) Ra=0,92

### 3.2 SEM Images

SEM analyzes were performed to analyze the surfaces obtained after deep rolling and to evaluate the surface morphology. First of all, for comparison purposes, a

finish turning operation was applied before deep rolling, and then SEM images of the surface were taken (Figure 11), thus, it was aimed to examine and compare it after deep rolling.

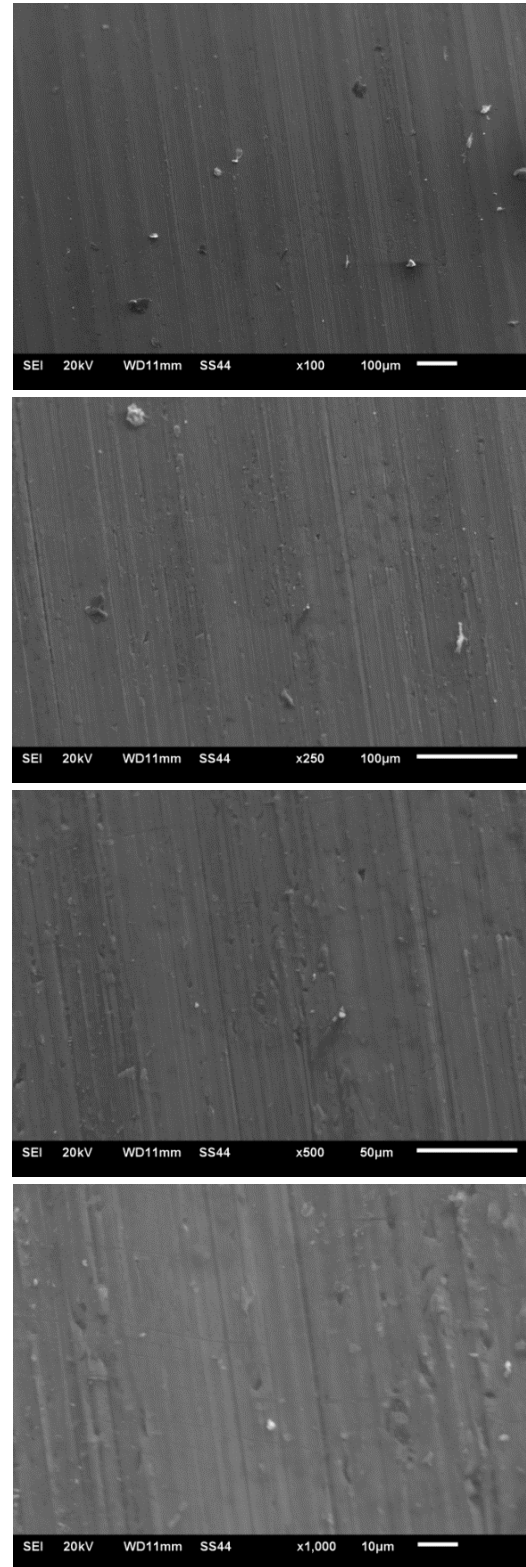


**Figure 11.** Images of deep-rolled finishing turning surfaces

In the deep rolling process, especially in the deep rolling of materials such as Al, it is seen that some particles (debris, BUE, etc.) are formed on the surface [46]. These debris can be seen in Figure 11. Here, the structures in Figure 12 were obtained in the SEM images taken to see the effect of the rolling force.

Depending on the increase in feed, it is seen that dents, scratches and residues on the surfaces increase (Figure 12).

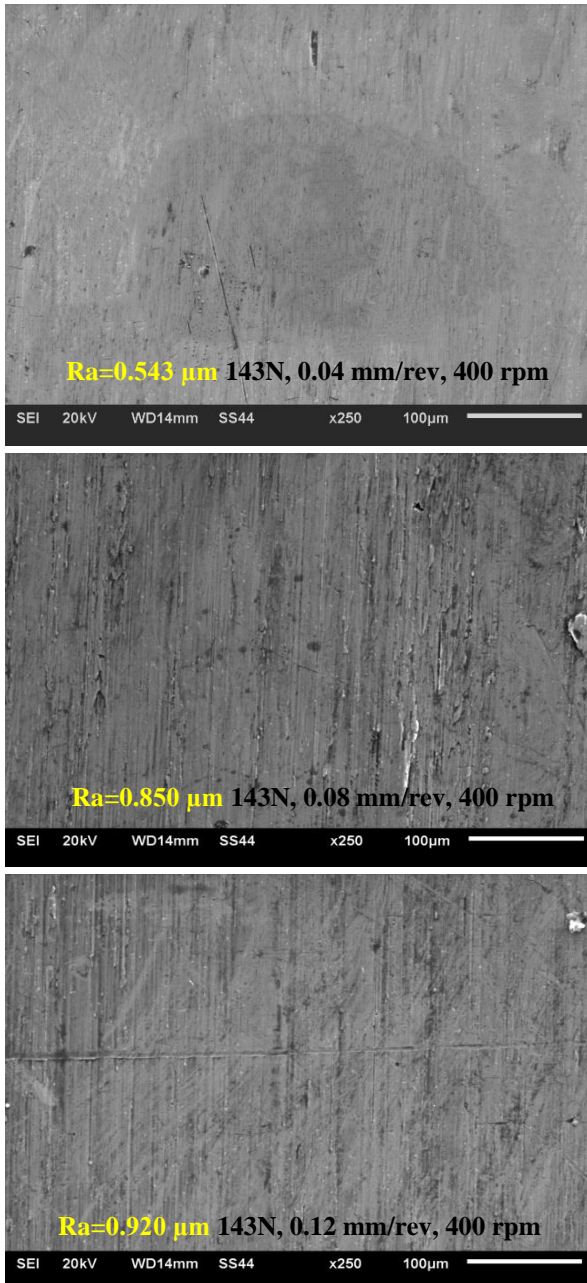


**Figure 12.** SEM images at a deep rolling force of 143 N

As a result of this situation, it is noted that there is an increase in Ra values. When the deep rolling mechanics are examined, it is seen that plastic deformation occurs

due to rolling. It is certain that this plastic deformation is shaped according to the process parameters, and deep rolling produces formations such as grooves and debris, and the surface topography arises depending on the effect of each parameter.

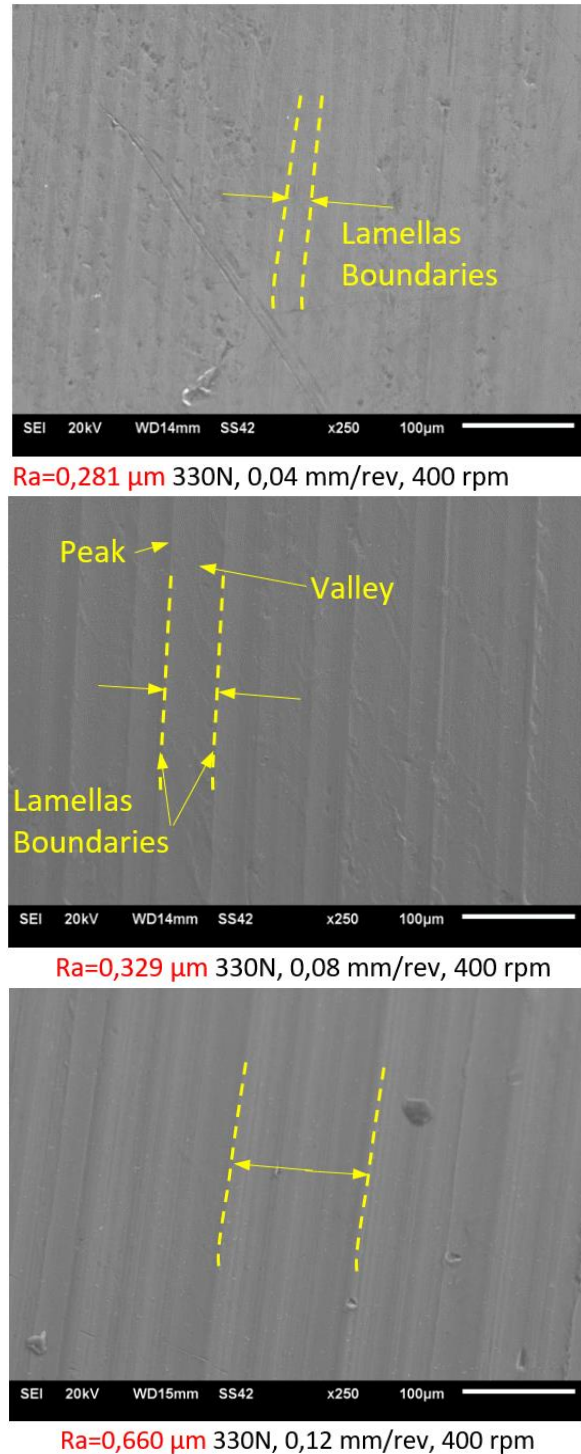


**Figure 13.** SEM images at 330 N rolling force

This is a type of process which is mechanically very complex, resulting from the type of material, friction behavior, heat, etc., and has not been proven by any

specific modeling yet. Although some results have been achieved in the studies, the subject has not yet been fully clarified. Therefore, much more work needs to be done. When the process was examined depending on the increase in rolling force, the structures in Figure 13 were obtained.

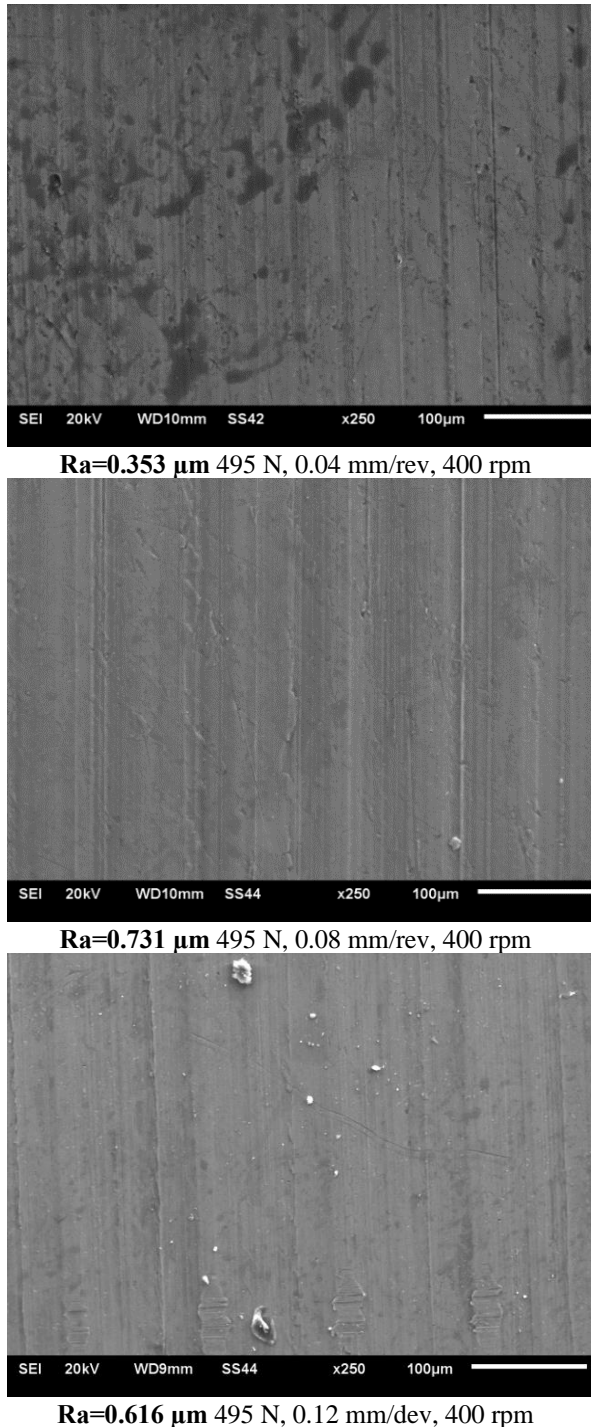


**Figure 14.** SEM images at a deep rolling force of 495 N

When both figure 12 and figure 13 are evaluated together, it can be seen that the surface topography has become more smooth, debris and grooves have decreased, and

accordingly, Ra values have decreased compared to 143 N rolling force. At 330 N rolling force, Ra values have increased depending on the increase in feed rate. In deep rolling, it is the pass in which the peaks remaining from the first finishing pass are filled into the valley parts with the first plastic deformation. The lower rolling force causes fewer peaks to be filled into valleys due to this pass. As the rolling force increases, the pressing force ensures that more material is filled into the valleys, resulting in the formation of a smoother surface. As a result, Ra values are further reduced. Due to the increase in feed, the increase in Ra also increases in parallel with that as in Figure 13. The most important issue that determines Ra values here is that the distance between the lamellar structure increases parallel to the feed rate, as seen in Figure 12, which is reflected in Ra values. SEM images with 495 N rolling force are given in Figure 14.

When the structures in Figure 12 and Figure 13 obtained with rolling forces of 143 N and 330 N are considered, it can be said that the rolling force of 330 N produces the best Ra values. Here, it was concluded that the increase in the rolling force causes excessive plastic deformation due to the increase in feed on the material surface, and the valleys on the surface are filled with more material than their volume causing deformations on the surface. At this point, Ra value, before deep rolling, appears as an important factor. Before the deep rolling process, it is necessary to determine Ra values and accordingly the peak and valley volumes and then determine the parameters of the deep rolling to be applied. In this regard, optimization studies are being carried out, and these should be done. There are studies showing the effectiveness of Ra values before deep rolling [32, 3].

#### 4. Conclusion

In this study, Al6061-T6 aluminum material was burnished by deep rolling method with a burnishing tip that can be used for conical, radius and cylindrical turning operations and can be fixed on the existing tool holder. The results obtained from the analyzes carried out to determine the relationship between microhardness, surface morphology and Ra in the deep rolling method of Al6061-T6 aluminum material can be summarized as follows:

- When the microhardness result was examined, it was revealed that the most ideal parameter on Ra was 495 N in rolling force, 0.08 mm/rev in feed and 400 rpm in speed.
- 200x optical microscope images of the workpieces were taken, thus it was seen that the images were distributed homogeneously.
- When SEM images are analyzed, it was observed that there was a decrease in Ra values due to the decrease in the distance between the lamellar structures with the increase in feed. This result is also compatible with the literature.

- Due to the increase in rolling pressure force and the increase in feed rate on the material surface, excessive plastic deformation occurred and the valleys on the surface were filled with more material than their volumes, causing deformations there. For this reason, the rolling force limit must be determined well.
- Due to the increase in feed, it was observed that debris, grooves and residues on the surfaces increased. Microhardness values were obtained at 140-160 HV<sub>0.03</sub> values and were observed to decrease with distance from the surface.
- It seems difficult to talk about a sufficient trend to reach a conclusion between microhardness and parameters, as in the literature. The issue should be studied and researched further.
- It was observed that there is an inverse proportion between the spindle speed and hardness.

It was concluded that it is an important problem that the optimum criteria for obtaining the desired surface properties have not yet been achieved in deep rolling and ball burnishing processes. Therefore, more research is needed to determine the correct process parameters for this issue.

#### Author's Contributions

**Oktay Adıyaman:** Conducted the experiment and result analysis, and then drafted and prepared the article.

**Feyza Aydın:** Assisted and supervised the study, as well as helped in manuscript preparation.

#### Ethics

There are no ethical issues after the publication of this manuscript.

#### Acknowledgement

In order to carry out the research, Batman University unit of BAP (Scientific Research Projects) provided financial support to this study numbered BTUBAP-2022-YL-05.

#### References

- [1]. Wandra, R., Prakash, C., Singh, S. 2022. Experimental investigation and optimization of surface roughness of  $\beta$ -Phase titanium alloy by ball burnishing assisted electrical discharge cladding for implant applications. *Materials Today: Proceedings*; 48, 975-980, doi: 10.1016/j.matpr.2021.06.070.
- [2]. Kinner-Becker, T., Zmich, R., Sölter, J., Meyer, D. 2021. Combined laser and deep rolling process as a means to study thermo-mechanical processes. *Procedia CIRP*; 102, 369-374, doi: 10.1016/j.procir.2021.09.063.
- [3]. Prabhu, P. R., Kulkarni, S. M., Sharma, S. S. 2011. An experimental investigation on the effect of deep cold rolling parameters on surface roughness and hardness of AISI 4140 steel. *World Academy of Science, Engineering and Technology*; 60, 1594-1598.

- [4]. Başak, H., Sönmez, F., 2015. In Burnishing Process, Inspection of The Burnishing Apparatus (Ball, Roller, Twist Roller) Effects on Surface Roughness and Surface Hardness, *Journal of Polytechnic*; 18(3), 125-132, doi: 10.2339/2015.18.3, 125-132.
- [5]. Mendi, F., Takım tezgâhları teori ve hesapları, ISBN:975-06008-0-3, Ankara, 1996.
- [6]. Özkan, S. 2006. Sürtünme karıştırma kaynağı ile birleştirilen parçalarda haddeleme (burnishing) ile yüzeylerin işlenmesi, haddelemenin yüzey pürüzlülüğüne ve sertleşmeye etkisinin incelenmesi. *M.S. thesis, Gazi Üniversitesi Fen Bilimleri Enstitüsü*, Ankara.
- [7]. Akyüz, M. 2020. Bilyeli haddeleme yönteminde işlem parametrelerinin Al7075-T6 alüminyum alaşımının mekanik özellikleri üzerindeki etkilerinin deneysel olarak araştırılması. *M.S. thesis, Fen Bilimleri Enstitüsü Fırat Üniversitesi*, Elazığ.
- [8]. Hassan A. D., Maqableh A. M., 2000. The effects of initial burnishing parameters on non-ferrous components. *Journal of Materials Processing Technology*; 102(1-3), 115-121, doi: 10.1016/S0924-0136(00)00464-7.
- [9]. Luo H., Wang L., Zhang C. 2011. Study on the aluminum alloy burnishing processing and the existence of the outstripping phenomenon. *Journal of Materials Processing Technology*; 116, 88-90, doi: 10.1016/S0924-0136(01)00847-0.
- [10]. Hassan, A. M. 1997. The effects of ball-and roller-burnishing on the surface roughness and hardness of some non-ferrous metals. *Journal of materials processing technology*; 72(3), 385-391, doi: 10.1016/S0924-0136(97)00199-4.
- [11]. Yu X., Wang L. 1999. Effect of various parameters on the surface roughness of an aluminium alloy burnished with a spherical surfaced polycrystalline diamond tool. *International Journal of Machine Tools & Manufacture*; 39(3), 459-469, doi: 10.1016/S0890-6955(98)00033-9.
- [12]. El-Axir, M.H., El-Khabeery, M.M. 2003. Influence of orthogonal burnishing parameters on surface characteristics for various materials. *Journal of Materials Processing Technology*; 132, 82-89, doi: 10.1016/S0924-0136(02)00269-8.
- [13]. Zhuang, W., Liu, Q., Djugum, R., Sharp, P.K., Paradowska, A. 2014. Deep surface rolling for fatigue life enhancement of laser clad aircraft aluminium alloy. *Applied Surface Science*; 320, 558-562, doi: 10.1016/j.apsusc.2014.09.139.
- [14]. Majzoobi, G.H., Jouneghani, F.Z., Khademi, E. 2016. Experimental and numerical studies on the effect of deep rolling on bending fretting fatigue resistance of Al7075. *Int. J. Adv. Manuf. Technol*; 82, 2137-2148, doi: 10.1007/s00170-015-7542-z.
- [15]. Khabeery M. M., Axir M. H., 2001. Experimental techniques for studying the effects of milling roller-burnishing parameters on surface integrity. *International Journal of Machine Tools & Manufacture*; 41(12), 1705-1719, doi: 10.1016/S0890-6955(01)00036-0.
- [16]. Basak H., Goktas H.H. 2009. Burnishing process on al-alloy and optimization of surface roughness and surface hardness by fuzzy logic. *Materials and Design*; 30, 1275-1281, doi: 10.1016/j.matdes.2008.06.063.
- [17]. Tadic B., Todorovic M. P., Luzanin O., Miljanic D., Jeremic M. B., Bogdanovic B., Vukelic D. 2013. Using specially designed high-stiffness burnishing tool to achieve high-quality surface finish. *The International Journal of Advanced Manufacturing Technology*; 67, 601-611, doi: 10.1007/s00170-012-4508-2.
- [18]. Akkurt, A., Ovalı, İ. 2009. The effects of burnishing and conventional finishing processes on surface roughness and roundness

of the Al 6061 aluminum parts. *Pamukkale Üniversitesi Mühendislik Bilimleri Dergisi*; 15(3), 371-382.

[19]. Akkurt, A. Delik yüzeylerine uygulanan yüzey iyileştirme işlemlerinin alüminyum alaşımı malzemeler üzerinde araştırılması, 5. Uluslararası İleri Teknolojiler Sempozyumu (IATS'09), Karabük, Turkey, 2009.

[20]. Başak, H. 2015. Haddeleme (Galetaj) ile 5083 Al-Mg malzeme yüzeyinin işlenmesi, haddeleme parametrelerinin yüzey pürüzlülüğü ve yüzey sertliğine etkilerinin incelenmesi. *GU J Sci Part:C*; 3(2), 471-476.

[21]. Malyer, E. 2018. Examining the residual stress on the burnished AA7075-T6 aluminum alloy. *Journal of Polytechnic*; 21(3), 565-573, doi: 10.2339/politeknik.389592.

[22]. Maiß, O., Röttger, K. 2022. Monitoring the surface quality for various deep rolling processes—limits and experimental results. *Procedia CIRP*; 108, 857-862, doi: 10.1016/j.procir.2022.05.199.

[23]. Oevermann, T., Wegener, T., Liehr, A., Hübner, L., Niendorf, T. 2021. Evolution of residual stress, microstructure and cyclic performance of the equiatomic high-entropy alloy CoCrFeMnNi after deep Rolling. *International Journal of Fatigue*; 153, 106513.

[24]. Martins, A. M. Leal, C. A. Campidelli, A. F. Abrao, A. M.; Rodrigues, P. C. Magalhães, F. C. Meyer, K. 2022. Assessment of the temperature distribution in deep rolling of hardened AISI 4140 steel. *Journal of Manufacturing Processes*; 73, 686-694, doi: 10.1016/j.jmapro.2021.11.052.

[25]. Bogachev, I., Knowles, K. M., Gibson, G. J. 2021. Deep cold rolling of single crystal nickel-based superalloy CMSX-4. *Materialia*; 20, 101240, 2021.

[26]. Hettig, M., Meyer, D. 2020. Sequential multistage deep rolling under varied contact conditions. *Procedia CIRP*; 87, 291-296, doi: 10.1016/j.procir.2020. 02.027.

[27]. Basak, H., Ozkan, M., Toktas, I. 2019. Experimental research and ANN modeling on the impact of the ball burnishing process on the mechanical properties of 5083 Al-Mg material. *Kovové materiály-Metallic Materials*; 57(1), 61-74, doi: 10.4149/km 2019\_1\_61.

[28]. Delgado, P., Cuesta, I. I., Alegre, J. M., Díaz, A. 2016. State of the art of Deep Rolling. *Precision Engineering*; 46, 1-10, doi: 10.1016/j.precisioneng.2016. 05.001.

[29]. Sönmez, F., Başak, H., Baday, Ş. 2016. Haddeleme işleminin yüzey yanıt yöntemi ile analizi. *Gazi University Journal of Science Part C: Design and Technology*, 4(4), 275-283.

[30]. Adıyaman, O. 2024. Investigation on the Application of Worn Cutting Tool Inserts as Burnishing Tools. *Strojniški vestnik - Journal of Mechanical Engineering*, 70(1-2), 92-102. doi:http://dx.doi.org/10.5545/sv-jme.2023.781

[31]. Blasón, S., Rodríguez, C., Belzunce, J., Suárez, C. 2017. Fatigue behaviour improvement on notched specimens of two different steels through deep rolling, a surface cold treatment. *Theoretical and Applied Fracture Mechanics*; 92, 223-228, doi: 10.1016/j.tafmec.2017.08.003.

[32]. Prabhu, P. R., Kulkarni, S. M., Sharma, S. 2020. Multi-response optimization of the turn-assisted deep cold rolling process parameters for enhanced surface characteristics and residual stress of AISI 4140 steel shafts”, *Journal of Materials Research and Technology*; 9(5), 11402-11423, doi: 10.1016/j.jmrt.2020.08.025

[33]. El-Axir, M. H., Othman, O. M., & Abodiena, A. M. 2008. Improvements in out-of-roundness and microhardness of inner surfaces by internal ball burnishing process. *Journal of materials processing technology*, 196(1-3), 120-128. doi: 0.1016/j.jmatprotec.2007.05.028

[34]. Aydın, F., Adıyaman, O. 2023. Experimental investigation of new type insert in deep rolling of al6061-t6 material. *Rahva Journal of Technical and Social Studies*; 3(1), 58-72.

[35]. Aydın, F., Adıyaman, O. 2023. Yeni tip insert uç ile Al6061 malzemeye bilyeli parlatma yöntemi uygulanması ve yüzey özelliklerinin incelenmesi. 2nd International Rahva Technical and Social Researches Congress, Bitlis, Turkey, 171-172.

[36]. Yüce Teknik, 2023, <https://www.yuceteknik.com/> Mekanik-Kalip-Yaylari-Yesil-Yay.PR-1779.html (accessed: 20/08/2023).

[37]. Technical Data Sheet, 2024, [https://www.skf.com/binaries/pub12/Images/LubriFluid\\_TD\\_US\\_tcm\\_12-158093.pdf](https://www.skf.com/binaries/pub12/Images/LubriFluid_TD_US_tcm_12-158093.pdf), (accessed :06/03/2024)

[38]. Lee SH. 2003. Optimization of cutting parameters for burr minimization in face-milling operations. *Int J Prod Res* 41 (3):497 doi:10.1080/0020754021000042382.

[39]. Lin TR (2002) Optimization technique for face milling stainless steel with multiple performance characteristics. *Int J Adv Manuf Technol* 19:330 doi:10.1007/s001700200021

[40]. Ross PJ (1996) Taguchi techniques for quality engineering, 2<sup>nd</sup> edn. McGraw-Hill, New York

[41]. El-Tayeb, N. S. M., Low K. O., Brevern P. V. 2007. Influence of roller burnishing contact width and burnishing orientation on surface quality and tribological behaviour of Aluminium 6061. *Journal of materials processing technology*; 186(3), 272-278, doi: 10.1016/j.jmatprotec.2006.12.044.

[42]. Egea A.J.S., Rodríguez A., Celentano D., A.Calleja, Lacalle L.N. 2019. Joining metrics enhancement when combining FSW and ball-burnishing in a 2050 aluminium alloy. *Surface & Coatings Technology*; 367, 327–335, doi: 10.1016/j.surfcoat.2019. 04.010.

[43]. Koçak, H. 2020. Improving the surface properties of Al 6013 and MS 58 materials by ball burnishing process for hole. *GU J Sci, Part C*; 8(4), 972-980, doi: 10.29109/gujsc.821576.

[44]. Martins, A. M., Oliveira, D. A. D., de Castro Magalhães, F., & Abrão, A. M. (2023). Relationship between surface characteristics and the fatigue life of deep rolled AISI 4140 steel. *The International Journal of Advanced Manufacturing Technology*, 129(3), 1127-1143. doi: 10.1007/s00170-023-12332-x.

[45]. Shetty, R., Rao, S. S., & Gaitonde, V. N. 2017. Wear resistance enhancement of titanium alloy (Ti-6Al-4V) by ball burnishing process. *Journal of Materials Research and Technology*, 6(1), 13-32. doi: 10.1016/j.jmrt.2016.03.007.

[46]. Wang, Z., Xiao, Z., Huang, C., Wen, L., & Zhang, W. 2017. Influence of ultrasonic surface rolling on microstructure and wear behavior of selective laser melted Ti-6Al-4V alloy. *Materials*, 10(10), 1203, doi: 10.3390/ma10101203.

[47]. Attabi, S., Himour, A., Laouar, L., & Motalebzadeh, A. 2021. Mechanical and wear behaviors of 316L stainless steel after ball burnishing treatment. *Journal of Materials Research and Technology*, 15, 3255-3267. doi: 10.1016/j.jmrt.2021.09.081.

[48]. Herbster, M., Harnisch, K., Haberland, E., Kriegel, P., Döbberthin, C., Heyn, A., Halle, T. 2021. Effect of deep rolling on subsurface conditions of CoCr28Mo6 wrought alloy to improve the wear resistance of endoprostheses. *Journal of the Mechanical Behavior of Biomedical Materials*; 118, 104398, doi: 10.1016/j.jmbbm.2021.104398.



- [49]. Chen, M., He, J., Wang, M., Li, J., Xing, S., Gui, K., Liu, Q. 2022. Effects of deep cold rolling on the evolution of microstructure, microtexture, and mechanical properties of 2507 duplex stainless steel. *Materials Science and Engineering: A*; 845, 143224. doi: 10.1016/j.msea.2022.143224.